Molecules and Cells

RIP3-Dependent Accumulation of Mitochondrial Superoxide Anions in TNF-α-Induced Necroptosis

Jiyoung Lee, Sunmi Lee, Seongchun Min*, and Sang Won Kang*

Department of Life Science, College of Natural Science, Ewha Womans University, Seoul 03760, Korea
*Correspondence: scmin922@ewha.ac.kr (SM); kangsw@ewha.ac.kr (SWK)
https://doi.org/10.14348/molcells.2021.0260
www.molcells.org

Excessive production of reactive oxygen species (ROS) is a key phenomenon in tumor necrosis factor (TNF)-α-induced cell death. However, the role of ROS in necroptosis remains mostly elusive. In this study, we show that TNF-α induces the mitochondrial accumulation of superoxide anions, not H_2O_2, in cancer cells undergoing necroptosis. TNF-α-induced mitochondrial superoxide anions production is strictly RIP3 expression-dependent. Unexpectedly, TNF-α stimulates NADPH oxidase (NOX), not mitochondrial energy metabolism, to activate superoxide production in the RIP3-positive cancer cells. In parallel, mitochondrial superoxide-metabolizing enzymes, such as manganese-superoxide dismutase (SOD2) and peroxiredoxin III, are not involved in the superoxide accumulation. Mitochondrial-targeted superoxide scavengers and a NOX inhibitor eliminate the accumulated superoxide without affecting TNF-α-induced necroptosis. Therefore, our study provides the first evidence that mitochondrial superoxide accumulation is a consequence of necroptosis.

Keywords: NADPH oxidase, necroptosis, superoxide anion, tumor necrosis factor-α

INTRODUCTION

Both apoptosis and necroptosis are forms of programmed cell death and are initiated by tumor necrosis factor (TNF)-α stimulation. A growing number of studies described molecular switches between the two programmed cell death types, such as receptor-interacting protein 3 (RIP3), a key molecule that determines specific necrosome formation in the case of TNF-α-induced necroptosis in a receptor-interaction protein 1 (RIP1)-dependent manner (Cho et al., 2009; He et al., 2009; Zhang et al., 2009). Upon TNF-α binding, the TNF receptor (TNFR) trimerizes and mediates either apoptosis via caspase 8 activation or necroptosis via RIP1-RIP3 interaction. During necroptosis, TNFR-mediated RIP1activation and phosphorylation leads to subsequent RIP3 phosphorylation through the RHIM domain. The RIP1-RIP3 complexes recruit and phosphorylate the downstream pseudo-kinase mixed lineage kinase domain-like to form a necrosome complex. Finally, the necrosome complexes translocate to the plasma membrane and cause membrane swelling and rupture (Tang et al., 2019; Vanden Berghe et al., 2014; Weinlich et al., 2017).

Reactive oxygen species (ROS) are highly reactive molecules including superoxide anion, hydrogen peroxide (H_2O_2), and hydroxyl radical. Two major ROS sources related to the TNF-α-induced cell death are NADPH oxidase (NOX) and mitochondria (Blaser et al., 2016; Morgan and Liu, 2010). It has long been thought that ROS play pivotal roles in TNF-α-induced cell death in various cell types. Nonetheless, the precise role of ROS in necroptosis is still debated.

In this study, we investigated this question using specific probes that distinguish specific ROS types. Unexpectedly, the cytosolic H_2O_2 was a major ROS type produced related to apoptosis, whereas mitochondrial superoxide accumulation was a key phenomenon in necroptosis. More interestingly,

Received 10 November, 2021; revised 29 November, 2021; accepted 10 December, 2021; published online 14 March, 2022

eISSN: 0219-1032

NOX was involved in mitochondrial superoxide production in necroptosis.

MATERIALS AND METHODS

Antibodies and reagents

Anti-human RIP3 (Cat. No. 13526) and anti-human SOD2 (Cat. No. 13194S) antibodies were purchased from Cell Signaling Technology (USA). Anti-mouse RIP3 antibody (Cat. No. NBP1-77299) was purchased from NOVUS Biologicals (USA). Anti-human PrxIII (Cat. No. LF-MA0045), anti-Prx-$SO_{2/3}$ (Cat. No. LF-PA0004), and anti-α-tubulin (Cat. No. LF-MA0117) antibodies were purchased from AbFrontier (Korea). HRP-conjugated rabbit IgG and mouse IgG antibodies were purchased from Bio-Rad (USA). Human TNF-α (Cat. No. PHC3016) was purchased from Gibco (USA). Hydrogen peroxide (Cat. No. H1009) and cycloheximide (Cat. No. C7698) were purchased from Sigma-Aldrich (USA). zVAD (Cat. No. 627610), BV6 (Cat. No. S7597), and MitoPY1 (Cat. No. 4428) were purchased from Calbiochem (USA), Selleckchem (USA), and TOCRIS (UK), respectively. MitoSOX Red (Cat. No. M36008) and dihydroethidium (Cat. No. D11347) were purchased from Invitrogen (USA).

Cell culture

HeLa, HT-29, NIH-3T3, and L929 cells were purchased from the American Type Culture Collection (USA). HeLa and L929 cells were cultured in Dulbecco's modified Eagle medium (DMEM) supplemented with 10% fetal bovine serum (Gibco), 100 units/ml of penicillin, 100 units/ml of streptomycin (Lonza, Switzerland). HT-29 cells were cultured in McCoy's 5A medium supplemented with 10% fetal bovine serum (Gibco), 100 units/ml of penicillin, 100 units/ml of streptomycin (Lonza). NIH-3T3 cells were cultured in DMEM supplemented with 10% calf bovine serum (Gibco), 100 units/ml of penicillin, 100 units/ml of streptomycin (Lonza). These cells were maintained at 37°C under an atmosphere of 5% CO_2.

RNA interference

The human and mouse RIP3-specific siRNA duplex sequences (5'-GCA GUU GUA UAU GUU AAC GAG CGG UCG-3' and 5'-AAG AUU AAC CAU AGC CUU CAC CUC CCA-3') were selected according to a previous study (Cho et al., 2009). The sequence-verified human SOD2-specific siRNA was purchased from Santa Cruz Biotechnology (USA). A control siRNA against firefly luciferase was purchased from Dharmacon (USA). The siRNA was transfected for 48 h using the LipoJet™ reagent (SignaGen, USA).

Measurement of intracellular ROS

Mitochondrial and cytosolic superoxide anion levels were determined using MitoSOX Red and dihydroethidium (DHE) (Molecular Probes, USA), respectively. The mitochondrial H_2O_2 level was assessed using MitoPY1 (Molecular Probes). Cells were cultured on 35-mm glass-bottom dishes and treated with either TNF-α (20 ng/ml) plus cycloheximide (10 μg/ml) or TNF-α plus BV6 (1 μM) in the presence of a pan-caspase inhibitor zVAD-fmk (20 μM) for apoptosis or necroptosis induction, repectively. After the stimulation, cells were rinsed once with Hanks' Balanced Salt Solution and incubated for 15 min with the indicated dyes. Fluorescence images were taken using a Zeiss LSM 880 confocal laser scanning microscope and analyzed using the Image J software.

Ratiometric imaging of cytosolic H_2O_2 was assessed using an H_2O_2-sensing and cytosol-targeted fluorescence protein called HyPer-Cyto (Evrogen, Russia). Cells were transfected with the plasmid vector encoding HyPer-Cyto for 16 h. After the transfection, the cells were treated with indicated stimuli. The fluorescence images were obtained with two excitation wavelengths at 405 nm and 488 nm. The fluorescence intensity ratios (F_{488}/F_{405}) represent the cytosolic H_2O_2 level.

Immunoblotting

Cells were lysed in a chilled lysis buffer containing 20 mM HEPES (pH 7.0), 150 mM NaCl, 10% glycerol, 1% Triton X-100, 2 mM EGTA, 1 mM EDTA, 5 mM Na_3VO_4, 5 mM NaF, 1 mM AEBSF, aprotinin (5 μg/ml), and leupeptin (5 μg/ml). The lysates were centrifuged for removing cell debris and nuclei. The protein concentration in the supernatant was measured using the Bradford assay. Proteins were resolved by SDS-PAGE and transferred onto nitrocellulose membranes by electroblotting. Immunoblot analysis was performed with specific antibodies following the standard protocol. The immune complexes with horseradish peroxidase-conjugated secondary antibodies were visualized by enhanced chemiluminescence on ChemiDoc imaging system (Bio-Rad).

Necroptotic cell death assay

Cells (2×10^5) were seeded onto 6-well plates and cultured for 24 h. Cells were treated with indicated stimuli for 6 h and then collected into a 5 ml FACS tube by pipetting. Then, the cells were centrifuged for 3 min, washed with cold phosphate-buffered saline (PBS). The final cell pellets were stained using Annexin V-FITC apoptosis detection kit I (BD Biosciences, USA). Cells were stained with Annexin V–FITC (BD Biosciences; Cat. No. 556419) for 20 min, then propidium iodide (Molecular Probes; Cat. No. P1304) for 5 min. The stained cells were analyzed using the FACS Calibur system (BD Biosciences).

SOD activity assay

Intracellular SOD activity was measured with a Colorimetric Assay Kit (BioVision, USA) using WST-1 according to the manufacturer's instructions. The washed cells were lysed in ice-cold 0.1 M Tris/HCl, pH 7.4 containing 0.5% Triton X-100, 5 mM β-ME, 0.1 mg/ml PMSF. Whole cell lysates (20 μl) were incubated with 200 μl of WST-1 working solution together with 20 μl of Enzyme Solution for 20 min at 37°C. WST-1 would be converted to WTS-1 formazan by remaining superoxide in assay solutions. The amount of formazan was measured at 450 nm using an Epoch™ 2 Microplate Spectrophotometer (BioTek, USA).

NADH/NAD assay

Cells (2×10^5) were seeded onto 6-well plates and cultured for 24 h. After the indicated stimulation, the cells were washed thrice with PBS and lysed with 50 μl of 0.2 N NaOH with 1% dodecyltrimethylammonium bromide (DTAB) solution. The

ratio of NAD^+/NADH was measured by the NAD/NADH-Glo assay kit (Promega, USA) according to the manufacturer's instructions. To measure the oxidized forms (NAD^+), 50 μl of lysate was incubated with 25 μl of 0.4 N HCl at 60°C for 15 min. The samples were then incubated at room temperature for 10 min and supplemented with 25 μl of 0.5 M Tris base for neutralization. To measure the reduced forms (NADH), 50 μl of lysate was heated at 60°C for 15 min and incubated at room temperature for 10 min. Then, 50 μl of 0.25 M Tris in 0.2 N HCl was added for neutralzation. The NAD^+ and NADH levels were measured individually using a luminometer (PerkinElmer, USA).

Statistics

All experiments were repeated at least three times. Data were analyzed with the Student's *t*-test for comparisons between two groups (IBM SPSS Statistics ver. 25; IBM, USA) to determine the statistically significance. *P* values < 0.05 were considered statistically significant.

RESULTS

Characterization of TNFα-induced ROS generation in apoptosis and necroptosis

To determine the type of ROS generated during necroptosis, we selected two RIP3-positive cell lines, HT-29 and L929, for necroptosis studies (Fig. 1A). We also used HeLa cells that undergo apoptosis upon TNF-α stimulation. Briefly, TNF-α plus cycloheximide (CHX) treatment induces apoptosis in HeLa cells. Treatment of either TNF-α plus a pan-caspase inhibitor z-VAD-fmk (T/Z combination) or TNF-α/z-VAD plus a SMAC mimetic BV6 (T/B/Z combination) induces necroptosis in murine L929 cells or human HT-29 cells, respectively. The stimulated cells were labeled with various ROS probes and subjected to time-lapse imaging on a confocal microscope. First, we measured the mitochondrial ROS level in two ways. Labeling with MitoSOX showed that the mitochondrial superoxide level was persistently increased in both HT-29 and L929 cells, not in the HeLa cells (Fig. 1B). In contrast, labeling with MitoPY1, monitoring the mitochondrial H_2O_2 level, showed no positive fluorescence signal in either of HT-29 and L929 cells, but a strong positive fluorescence signal increase in HeLa cells that underwent apoptosis (Fig. 1C). Then, we measured the cytosolic ROS level similarly in two ways. Labeling with DHE monitoring the cytosolic superoxide level showed a broad superoxide level increase in both the HT-29 and L929, not HeLa cells (Fig. 1D). Inversely, HyPer-cyto protein expression, a cytosolic-targeted green fluorescent protein variant that monitors the cytosolic H_2O_2 level (Belousov et al., 2006), indicated a strong H_2O_2 level increase in the cytosol of HeLa, but not HT-29 and L929 cells that underwent necroptosis (Fig. 1E, Supplementary Fig. S1A). Taken together, we concluded that necroptosis and apoptosis involve the differential production of superoxide and H_2O_2 in the mitochondria.

Mitochondrial superoxide production is RIP3-dependent

Since we reported the role of cytosolic H_2O_2 in the apoptosis (Lee et al., 2019), we were interested in the role of mitochondrial ROS during necroptosis. Several studies have previously shown that RIP3 affects in the TNF-induced necroptosis and ROS generation (He et al., 2009; Zhang et al., 2009). Therefore, we examined the mitochondrial superoxide level in the RIP3-depleted HT-29 cells (Fig. 2A). RIP3 knockdown reduced indeed necroptosis in HT-29 cells stimulated with T/B/Z combination (Fig. 2B) as well as in L929 cells stimulated with T/Z combination (Supplementary Fig. S1B). Subsequently, the RIP3 knockdown also suppressed the TNF-α-induced mitochondrial superoxide production, measured by MitoSOX (Figs. 2C and 2D). Therefore, the data indicated that RIP3 is essential for necroptosis-related mitochondrial superoxide production.

NADPH oxidase produces the mitochondrial superoxide anion

A recent study showed that the RIP3-dependent aerobic respiration enhancement contributed to cellular ROS levels in T/Z combination-stimulated cancer cells (Yang et al., 2018). Therefore, we measured the NADH/NAD^+ ratio, to assess the mitochondrial respiration state (Stein and Imai, 2012), in the HT-29 cells that underwent necroptosis. As shown in Fig. 3A, the NADH/NAD^+ ratio was unchanged during necroptosis, suggests that mitochondrial energy metabolism was not responsible for TNF-α-induced necroptosis. Accordingly, we decided to test another ROS source called NOX, catalyzing the electron transfer from NADP`H to molecular oxygen for superoxide anion generation. We used a pan-NOX inhibitor named APX-115 (Cha et al., 2017; Joo et al., 2016) for this experiment. Indeed, APX-115 completely abrogated the mitochondrial superoxide production in T/B/Z combination-stimulated HT-29 cells (Figs. 3B and 3C). As NOX4 is a mitochondrial isoform (Block et al., 2009), APX-115 might target NOX4 in the mitochondria of HT-29 cells.

We further addressed whether the superoxide-metabolizing enzyme present in mitochondria could be involved in mitochondrial superoxide accumulation. Firstly, we examined the activity or status of manganese-superoxide dismutase (Mn-SOD, also called SOD2) that catalyzes the dismutation of superoxide anion to H_2O_2 (Wang et al., 2018). We observed neither cellular SOD2 level nor total SOD activity alteration in HT-29 cells upon T/B/Z combination (Supplementary Figs. S2A and S2B). However, the SOD2 knockdown increased the mitochondrial superoxide level (Supplementary Figs. S2C and S2D), confirming that the mitochondrial ROS in necroptosis is indeed the superoxide anion.

The superoxide anion is a short-lived free radical and it is spontaneously or enzymatically converted to H_2O_2 in the cytosol as well as in the mitochondria. Since SOD2 was intact, the accumulated superoxide anions are constantly converted to H_2O_2 molecules in the mitochondria, which are in turn reduced to water by the mitochondrial peroxidase peroxiredoxin (Prx) type III (Chang et al., 2004). Since Prx enzymes are inactivated by hyperoxidation during repeated reaction cycles, we then examined the Prx enzymes status using a specific antibody recognizing the hyperoxidized form of the Prx enzymes, designated as the Prx sulfinic/sulfonic form (Prx-$SO_{2/3}$) (Woo et al., 2003). As a result, the hyperoxidized Prx enzymes were not present in the HT-29 and L929 cells that underwent necroptosis, although they were detected in the

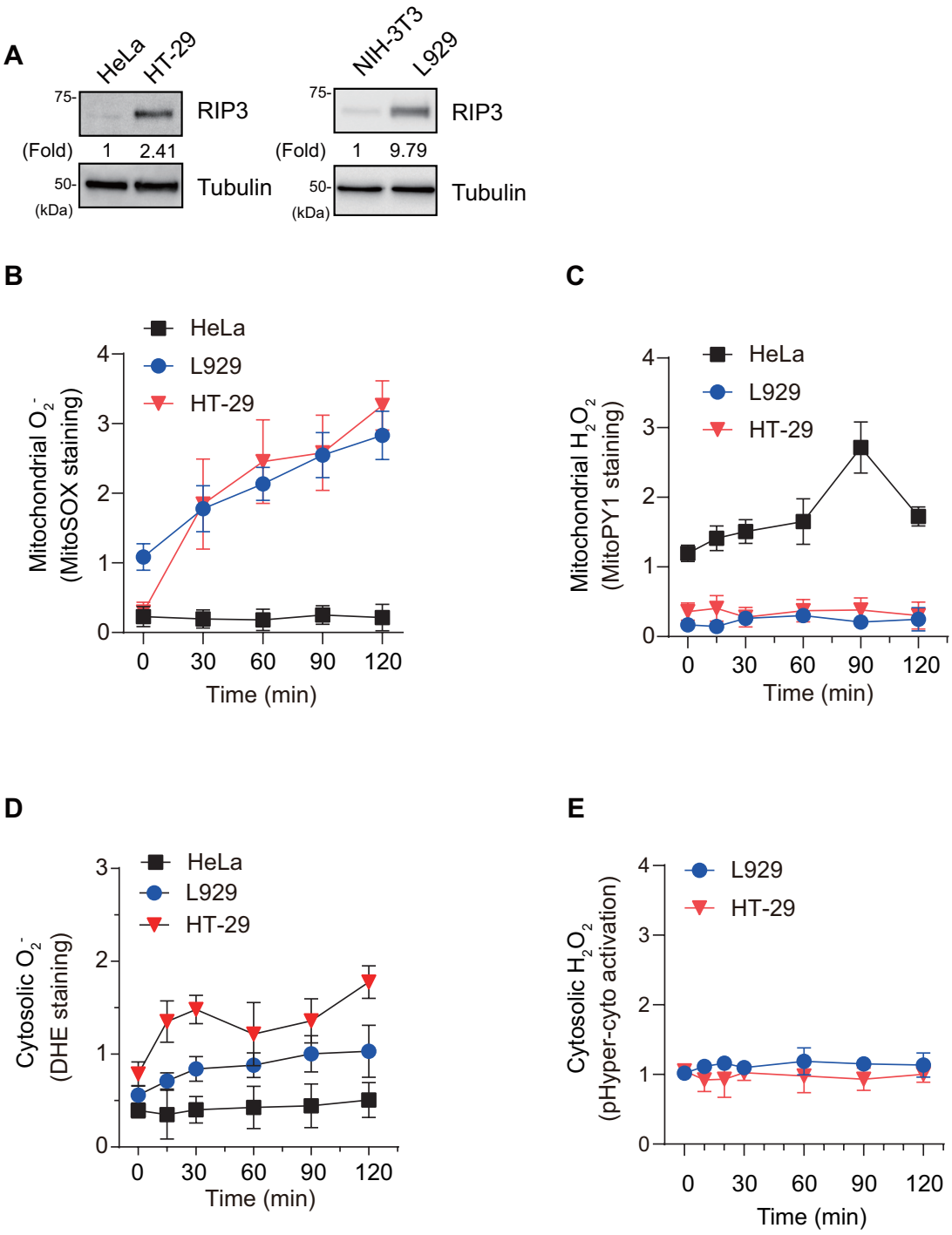

Fig. 1. Different types of ROS are produced in TNF-α-induced apoptosis and necroptosis. (A) Level of RIP3 protein expression in human cancer cells (HeLa and HT-29) and murine fibroblast cells (NIH-3T3 and L929). Immunoblots against α-tubulin as a loading control. Relative band intensities are quantified and shown as average of fold changes versus that of HeLa or NIH-3T3 cells, respectively (n = 2). (B-D) Intracellular ROS level was determined by indicated oxidation-sensitive probes. For induction of necroptosis, HT-29 and L929 cells were treated with TNF-α (10 ng/ml)/BV6 (1 μM)/zVAD (20 μM), abbreviated as T/B/Z, and TNF-α (10 ng/ml)/zVAD (20 μM) combination, respectively. For apoptosis, HeLa cells were treated with TNF-α (10 ng/ml) plus cycloheximide (10 μg/ml) combination. Data in the graph are means ± SD of fluorescence intensities of 100-150 cells from three independent experiments. Mitochondrial superoxide anion and H_2O_2 levels were measured using MitoSOX (B) and MitoPY1 (C), respectively. Level of cytosolic superoxide anion was measured using DHE (D). (E) Cytosolic H_2O_2 level was measured in the HyPer-expressing cells. Fluorescence images were taken from the HyPer-expressing HT-29 and L929 cells. Data in the graph are means ± SD of fold change of ratio of fluorescence intensities at 488 nm and 405 nm of 100-120 cells from three independent experiments.

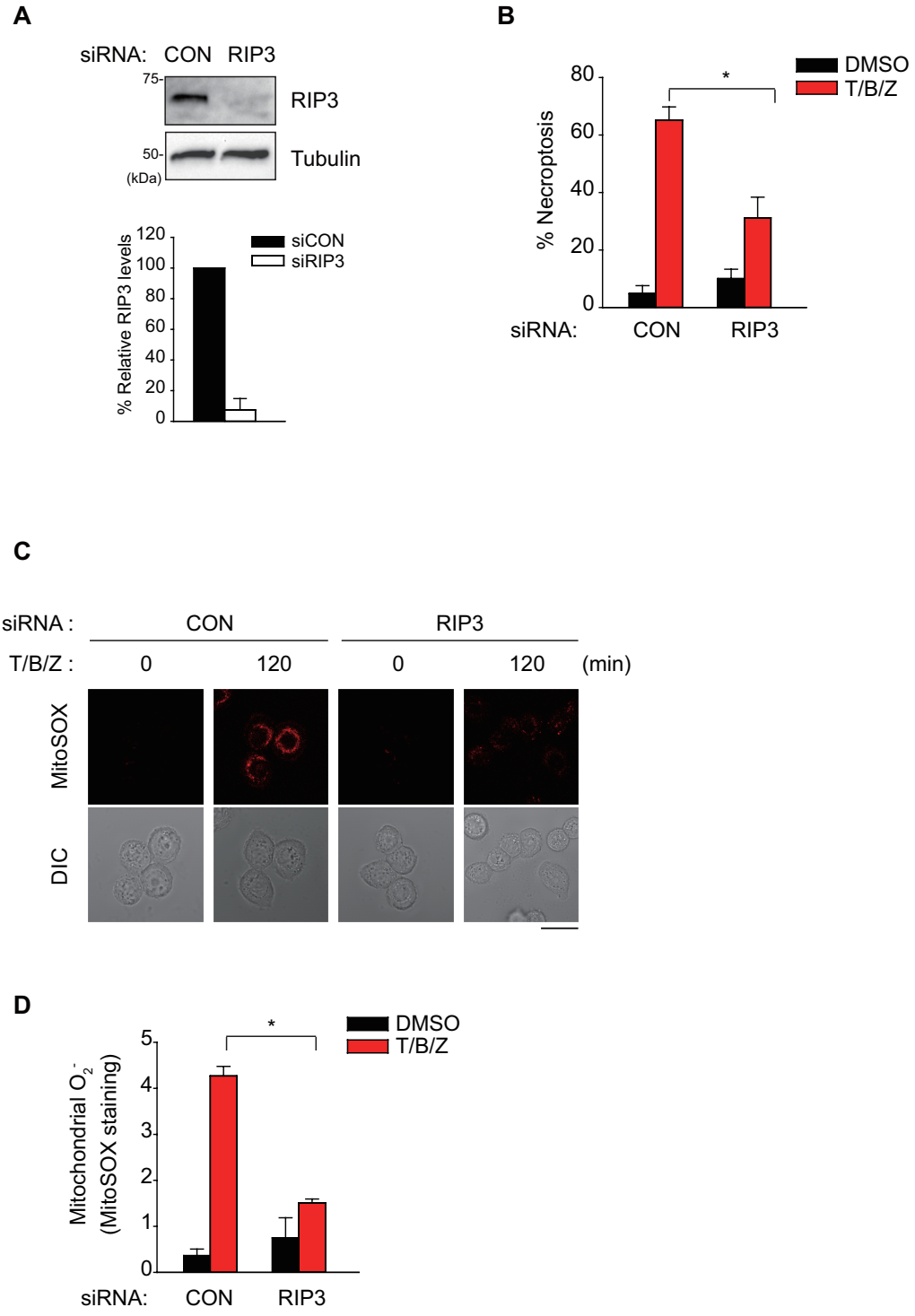

Fig. 2. RIP3 depletion attenuates mitochondrial superoxide anion production and necroptosis in HT-29 cells. (A) Knockdown of RIP3 expression in HT-29 cells by siRNAs specific to human RIP3. Level of RIP3 was shown by immunoblotting. Control siRNA (CON) is against firefly luciferase. Data in the graph are means of the percentage of ralative intensity of RIP3 band after being normailized by corresponding α-tubulin bands (n = 3). (B) The siRNA-transfected HT29 cells were treated with DMSO or TNF-α/BV6/zVAD (T/B/Z) combination for 6 h. The cells were labeled with propidium iodide (PI) and annexin-V followed by fluorescence-activated cell sorting (FACS) analysis. Data in the graph are means ± SD of the percentage of necroptotic cells (n = 3, $*P < 0.005$). (C and D) The siRNA-transfected HT-29 cells were treated with vehicle control (DMSO) or T/B/Z for 2 h and stained with MitoSOX. The flurescence (C) was analyzed by a confocal microscopy. Data in the graph are means ± SD of relative fluorescence intensities of 45 cells from three independent experiments ($*P < 0.001$). Scale bar = 20 μm.

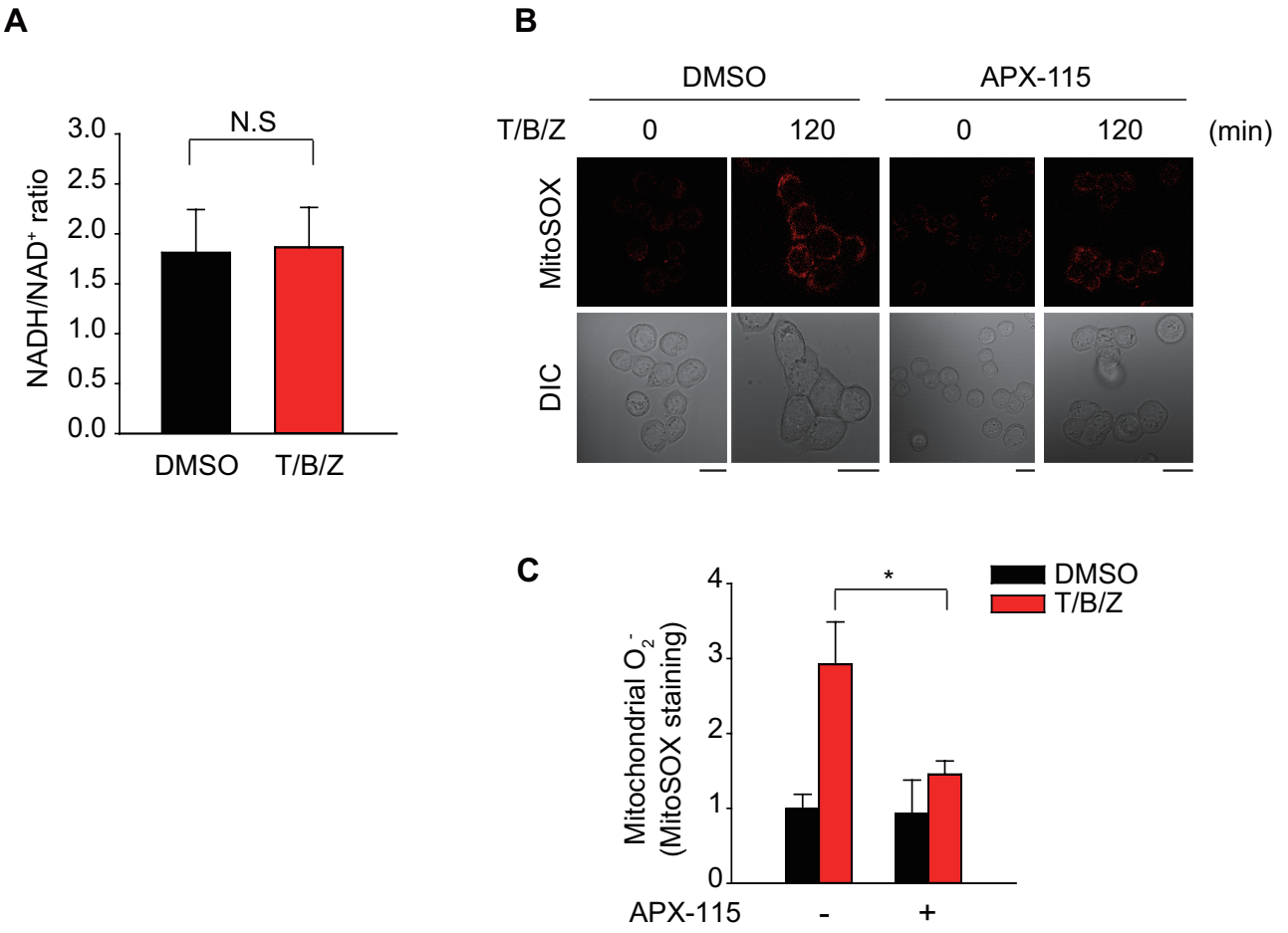

Fig. 3. NOX produces mitochondrial superoxide anion in the necroptosis. (A) Ratio of the reduced forms (NADH) to the oxidized forms (NAD^+) was determined in HT-29 cells treated with vehicle control (DMSO) or T/B/Z for 2 h. Data in the graph are means ± SD of luminoscence intensities averaged from triplicate wells (n = 3). N.S, not significant. (B and C) HT-29 cells were pretreated with vehicle control (DMSO) or APX-115 (10 μM) for 1 h and stimulated with T/B/Z for 2 h. Cells were stained with Mitosox and analyzed by a confocal microscopy. Data in the graph are means ± SD of relative fluorescence intensities of 100-120 cells (n = 3, $*P < 0.05$). A representative fluorescence image is shown (B). Scale bars = 20 μm.

same cells exogenously treated with a bolus of H_2O_2 solution at a micromolar concentration (Supplementary Fig. S2E). Taken together, the results showed that the mitochondrial ROS-metabolizing systems function well.

Mitochondrial superoxide accumulation is a result of necroptosis

A major question was whether mitochondrial superoxide accumulation is a cause or result of necroptosis. To better understand the role of mitochondrial superoxide in necroptosis, we pre-treated the HT-29 cells with various ROS inhibitors and performed a necroptosis assay. First, we applied chemical ROS scavengers, such as Necrox-2 and Mito-Tempo, which specifically eliminate the mitochondrial superoxide anion (Dikalova et al., 2010; Kim et al., 2010). Necrox-2 and or Mito-Tempo treatments indeed completely eliminated the mitochondrial superoxide level in T/B/Z combination-stimulated HT-29 cells (Figs. 4A and 4B). Nonetheless, neither chemicals affected the TNF-α-induced necroptosis in the HT-29 and L929 cells (Fig. 4C). To further confirm that, we used a pan-NOX inhibitor APX-115, which still did not affect TNF-α-induced necroptosis in either HT-29 or L929 cells (Figs. 4D and 4E). Finally, we examined necroptosis in SOD2-depleted HT-29 cells. SOD2 knockdown did not affect the TNF-α-induced necroptosis in the HT-29 cells (Fig. 4F). Overall, we concluded that the mitochondrial superoxide accumulation is a consequence of necroptosis.

DISCUSSION

Accumulating data indicate that ROS levels correlate with the caspase-independent cell death pathway (Dixon and Stockwell, 2014; Kim et al., 2007; Yang et al., 2018; Zhang et al., 2017; Zhao et al., 2012). In particular, TNF-α-induced necroptosis involves excessive ROS production. However, where and how ROS regulates necroptosis remain mostly uncharacterized. Recently, we demonstrated that the cytosolic H_2O_2 acts a signaling messenger role in TNF-α-induced apoptosis.

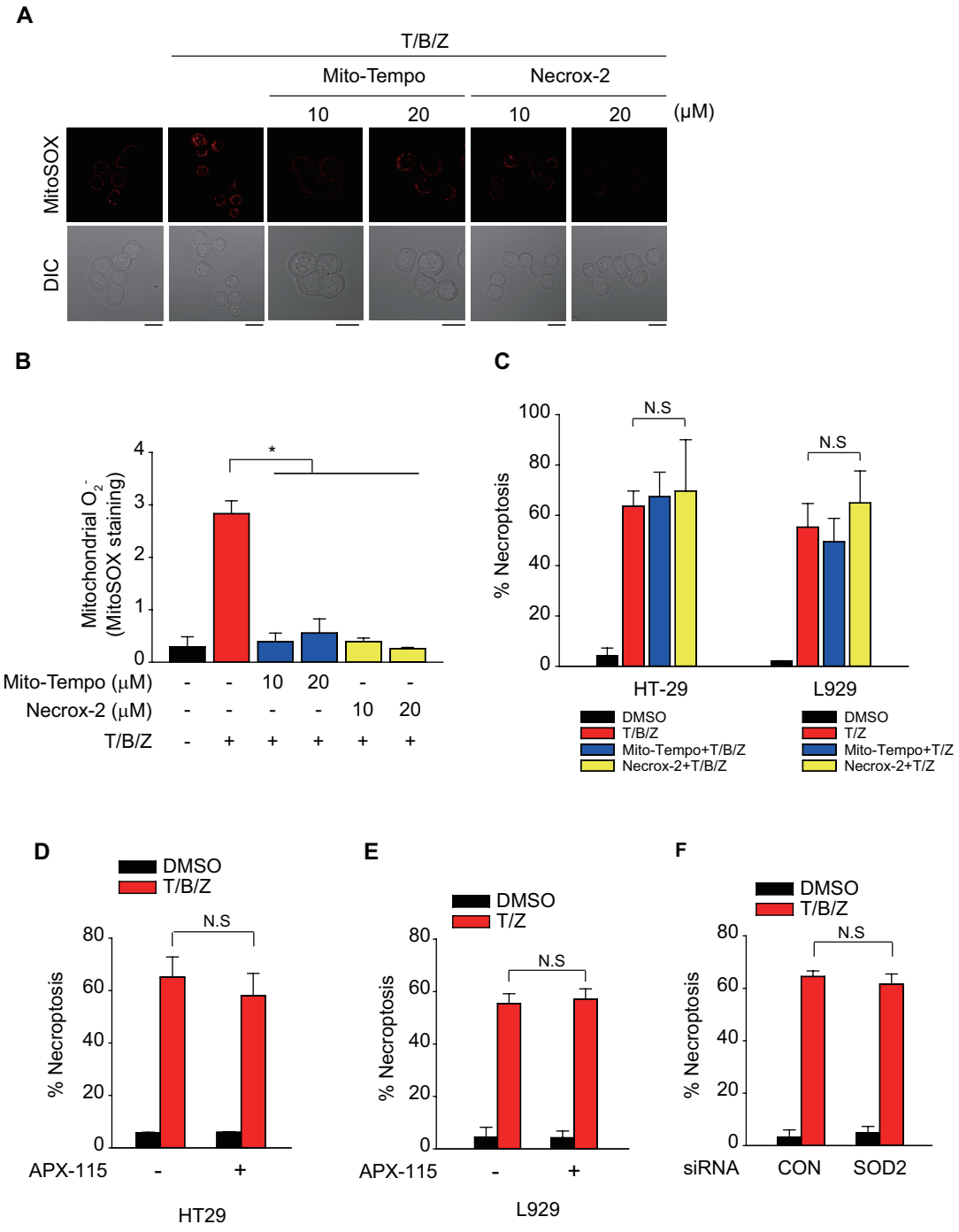

Fig. 4. Necroptosis accompanies with superoxide accumulation in the mitochondria. (A and B) HT-29 cells were pretreated with vehicle control (DMSO) or mitochondrial ROS scavengers (Mito-tempo [20 μM] and Necrox-2 [20 μM]) for 1 h and stimulated with T/B/Z for 2 h. Cells were stained with MitoSOX and analyzed by a confocal microscopy (A). Data in the graph are means ± SD of relative fluorescence intensities of 45-50 cells (n = 3, $*P < 0.001$). A representative fluorescence image is shown (A). Scale bars = 20 μm. DIC, differential interference contrast. (C) HT-29 and L929 cells were pretreated with vehicle control (DMSO) or mitochondrial ROS scavengers (Mito-tempo and Necrox-2) for 1 h and stimulated with T/B/Z and T/Z combination for 6 h, respectively. The cells were labeled with propidium iodide (PI) and annexin-V followed by FACS analysis. Data in the graph are means ± SD of the percentage of necroptotic cells (n = 3, N.S, not significant). (D and E) HT-29 and L929 cells were pretreated with vehicle control (DMSO) or APX-115 (10 μM) for 1 h and stimulated with combination of T/B/Z and T/Z for 6 h, respectively. The cells were labeled with PI and annexin-V followed by FACS analysis. Data in the graph are means ± SD of the percentage of necroptotic cells (n = 3, N.S, not significant). (F) The siRNA-transfected HT-29 cells were treated with vehicle control (DMSO) or T/B/Z combination for 6 h. Data in the graph are means ± SD of the percentage of necroptotic cells (n = 3, N.S, not significant). CON, control.

In that study, we risen the cytosolic H_2O_2 level by cellular thiol peroxidases, Prx and glutathione peroxidase (Gpx), depletion. These two peroxidase enzymes eliminate cellular H_2O_2 by utilizing the NADPH-derived reducing power (Kang and Kang, 2013; Veal et al., 2007). Specifically, Prx type I depletion increased DNA damage-dependent apoptosis, whereas that of Prx type II enhanced c-IAP/caspase-8 activation (Lee et al., 2019). More interestingly, Gpx1 depletion promoted apoptosis-inducing kinase 1 (ASK1)/c-Jun N-terminal kinase (JNK) pathways (Lee et al., 2021). Therefore, we interpreted that cytosolic H_2O_2 is an essential apoptosis signaling messenger. Since then, we decided to characterize necrosis-associated ROS level and type. For the first time, our data revealed mitochondrial superoxide anions accumulation in RIP3-positive cancer cells that underwent the TNF-α-induced necroptosis. Unlike the cytosolic H_2O_2 executing apoptosis, the mitochondrial superoxide did not execute necroptosis. Our results are consistent with those of previous studies showing that ROS production is dispensable in necroptosis of several cell types (He et al., 2009; Tait et al., 2013). However, it is potentially conceivable that the increased mitochondrial superoxide is involved in the release of damage-associated molecular pattern (DAMP), such as TNF, interleukin, or mtDNA, from damaged cells. Recent studies indicated that necroptosis could be a physiological endogenous inducer of inflammatory response via RIP3-dependent release of DAMPs during necroptotic cell death, and mitochondrial oxidative stress liberates mitochondrial DNA into the cytosol in which the interferon-dependent inflammatory response is triggered via the cGAS-STING pathway (Kim et al., 2019; Seong et al., 2020; Silke et al., 2015). Therefore, the accumulated superoxide anions within the mitochondria might be necessary for the release of pro-inflammatory factors such as mtDNA.

Our data also provide a key evidence of the fact that ROS types are different between apoptosis and necroptosis. The superoxide anion is a short-lived free radical, immediately converted to H_2O_2 by SOD (Imlay, 2008; Wang et al., 2018). Therefore, it was surprising that superoxide anions accumulated in the mitochondria of necroptotic cancer cells, where SOD2 and Prx type III are intact and abundant. However, we showed that mitochondrial superoxide production is mediated by the NOX enzyme, not the NADH-dependent respiratory energy metabolism, during TNF-induced necroptosis. Although NOX4 is known as a constitutively-active isoform in mitochondria (Block et al., 2009), we could not exclude the existence of a regulatory mechanism underlying the mitochondrial NOX activity enhancement by necroptosis.

In summary, the uniqueness of our study is live-cell imaging using various ROS-sensing probes to analyze the nature and localization of ROS in the necroptotic cells. As a result, our data demonstrated that superoxide anion, not H_2O_2, levels robustly increased in the mitochondria of RIP3-positive cancer cells undergoing necroptosis. This is a significant contrast to the robust increase of cytosolic H_2O_2 in TNF-α-induced apoptosis. Hence, the mitochondrial superoxide accumulation can be a useful marker of necroptosis.

Note: Supplementary information is available on the Molecules and Cells website (www.molcells.org).

ACKNOWLEDGMENTS

We thank Prof. Yun Soo Bae (Ewha Womans University) for sharing APX-115 reagent. This study was supported by grants from the National Research Foundation of Korea (2018R1A2B3006323 and 2017M3A9B6073098). S.M. was also supported by grants from the National Research Foundation of Korea (2019R1I1A1A01057557) and the RP-Grant (2019-2020) of Ewha Womans University.

AUTHOR CONTRIBUTIONS

J.L. and S.L. performed experiments. J.L., S.L., S.M., and S.W.K. designed experiments and analyzed the data. S.W.K. conceived the study and interpreted data. J.L., S.M., and S.W.K. wrote the manuscript.

CONFLICT OF INTEREST

The authors have no potential conflicts of interest to disclose.

ORCID

Jiyoung Lee https://orcid.org/0000-0001-6468-4366
Sunmi Lee https://orcid.org/0000-0002-6477-7316
Seongchun Min https://orcid.org/0000-0001-9410-5767
Sang Won Kang https://orcid.org/0000-0001-6446-163X

REFERENCES

Belousov, V.V., Fradkov, A.F., Lukyanov, K.A., Staroverov, D.B., Shakhbazov, K.S., Terskikh, A.V., and Lukyanov, S. (2006). Genetically encoded fluorescent indicator for intracellular hydrogen peroxide. Nat. Methods *3*, 281-286.

Blaser, H., Dostert, C., Mak, T.W., and Brenner, D. (2016). TNF and ROS crosstalk in inflammation. Trends Cell Biol. *26*, 249-261.

Block, K., Gorin, Y., and Abboud, H.E. (2009). Subcellular localization of Nox4 and regulation in diabetes. Proc. Natl. Acad. Sci. U. S. A. *106*, 14385-14390.

Cha, J.J., Min, H.S., Kim, K.T., Kim, J.E., Ghee, J.Y., Kim, H.W., Lee, J.E., Han, J.Y., Lee, G., Ha, H.J., et al. (2017). APX-115, a first-in-class pan-NADPH oxidase (Nox) inhibitor, protects db/db mice from renal injury. Lab. Invest. *97*, 419-431.

Chang, T.S., Cho, C.S., Park, S., Yu, S., Kang, S.W., and Rhee, S.G. (2004). Peroxiredoxin III, a mitochondrion-specific peroxidase, regulates apoptotic signaling by mitochondria. J. Biol. Chem. *279*, 41975-41984.

Cho, Y.S., Challa, S., Moquin, D., Genga, R., Ray, T.D., Guildford, M., and Chan, F.K. (2009). Phosphorylation-driven assembly of the RIP1-RIP3 complex regulates programmed necrosis and virus-induced inflammation. Cell *137*, 1112-1123.

Dikalova, A.E., Bikineyeva, A.T., Budzyn, K., Nazarewicz, R.R., McCann, L., Lewis, W., Harrison, D.G., and Dikalov, S.I. (2010). Therapeutic targeting of mitochondrial superoxide in hypertension. Circ. Res. *107*, 106-116.

Dixon, S.J. and Stockwell, B.R. (2014). The role of iron and reactive oxygen species in cell death. Nat. Chem. Biol. *10*, 9-17.

He, S., Wang, L., Miao, L., Wang, T., Du, F., Zhao, L., and Wang, X. (2009). Receptor interacting protein kinase-3 determines cellular necrotic response to TNF-alpha. Cell *137*, 1100-1111.

Imlay, J.A. (2008). Cellular defenses against superoxide and hydrogen peroxide. Annu. Rev. Biochem. *77*, 755-776.

Joo, J.H., Huh, J.E., Lee, J.H., Park, D.R., Lee, Y., Lee, S.G., Choi, S., Lee, H.J., Song, S.W., Jeong, Y., et al. (2016). A novel pyrazole derivative protects from ovariectomy-induced osteoporosis through the inhibition of NADPH oxidase. Sci. Rep. *6*, 22389.

Kang, D.H. and Kang, S.W. (2013). Targeting cellular antioxidant enzymes for treating atherosclerotic vascular disease. Biomol. Ther. (Seoul) *21*, 89-96.

Kim, H.J., Koo, S.Y., Ahn, B.H., Park, O., Park, D.H., Seo, D.O., Won, J.H., Yim, H.J., Kwak, H.S., Park, H.S., et al. (2010). NecroX as a novel class of mitochondrial reactive oxygen species and $ONOO^-$ scavenger. Arch. Pharm. Res. *33*, 1813-1823.

Kim, J., Gupta, R., Blanco, L.P., Yang, S., Shteinfer-Kuzmine, A., Wang, K., Zhu, J., Yoon, H.E., Wang, X., Kerkhofs, M., et al. (2019). VDAC oligomers form mitochondrial pores to release mtDNA fragments and promote lupus-like disease. Science *366*, 1531-1536.

Kim, Y.S., Morgan, M.J., Choksi, S., and Liu, Z.G. (2007). TNF-induced activation of the Nox1 NADPH oxidase and its role in the induction of necrotic cell death. Mol. Cell *26*, 675-687.

Lee, S., Lee, E.K., Kang, D.H., Lee, J., Hong, S.H., Jeong, W., and Kang, S.W. (2021). Glutathione peroxidase-1 regulates ASK1-dependent apoptosis via interaction with TRAF2 in RIPK3-negative cancer cells. Exp. Mol. Med. *53*, 1080-1091.

Lee, S., Lee, J.Y., Lee, E.W., Park, S., Kang, D.H., Min, C., Lee, D.J., Kang, D., Song, J., Kwon, J., et al. (2019). Absence of cytosolic 2-Cys Prx subtypes I and II exacerbates TNF-alpha-induced apoptosis via different routes. Cell Rep. *26*, 2194-2211.e6.

Morgan, M.J. and Liu, Z.G. (2010). Reactive oxygen species in TNFalpha-induced signaling and cell death. Mol. Cells *30*, 1-12.

Seong, D., Jeong, M., Seo, J., Lee, J.Y., Hwang, C.H., Shin, H.C., Shin, J.Y., Nam, Y.W., Jo, J.Y., Lee, H., et al. (2020). Identification of MYC as an antinecroptotic protein that stifles RIPK1-RIPK3 complex formation. Proc. Natl. Acad. Sci. U. S. A. *117*, 19982-19993.

Silke, J., Rickard, J.A., and Gerlic, M. (2015). The diverse role of RIP kinases in necroptosis and inflammation. Nat. Immunol. *16*, 689-697.

Stein, L.R. and Imai, S. (2012). The dynamic regulation of NAD metabolism in mitochondria. Trends Endocrinol. Metab. *23*, 420-428.

Tait, S.W., Oberst, A., Quarato, G., Milasta, S., Haller, M., Wang, R., Karvela, M., Ichim, G., Yatim, N., Albert, M.L., et al. (2013). Widespread mitochondrial depletion via mitophagy does not compromise necroptosis. Cell Rep. *5*, 878-885.

Tang, D., Kang, R., Berghe, T.V., Vandenabeele, P., and Kroemer, G. (2019). The molecular machinery of regulated cell death. Cell Res. *29*, 347-364.

Vanden Berghe, T., Linkermann, A., Jouan-Lanhouet, S., Walczak, H., and Vandenabeele, P. (2014). Regulated necrosis: the expanding network of non-apoptotic cell death pathways. Nat. Rev. Mol. Cell Biol. *15*, 135-147.

Veal, E.A., Day, A.M., and Morgan, B.A. (2007). Hydrogen peroxide sensing and signaling. Mol. Cell *26*, 1-14.

Wang, Y., Branicky, R., Noe, A., and Hekimi, S. (2018). Superoxide dismutases: dual roles in controlling ROS damage and regulating ROS signaling. J. Cell Biol. *217*, 1915-1928.

Weinlich, R., Oberst, A., Beere, H.M., and Green, D.R. (2017). Necroptosis in development, inflammation and disease. Nat. Rev. Mol. Cell Biol. *18*, 127-136.

Woo, H.A., Kang, S.W., Kim, H.K., Yang, K.S., Chae, H.Z., and Rhee, S.G. (2003). Reversible oxidation of the active site cysteine of peroxiredoxins to cysteine sulfinic acid. Immunoblot detection with antibodies specific for the hyperoxidized cysteine-containing sequence. J. Biol. Chem. *278*, 47361-47364.

Yang, Z., Wang, Y., Zhang, Y., He, X., Zhong, C.Q., Ni, H., Chen, X., Liang, Y., Wu, J., Zhao, S., et al. (2018). RIP3 targets pyruvate dehydrogenase complex to increase aerobic respiration in TNF-induced necroptosis. Nat. Cell Biol. *20*, 186-197.

Zhang, D.W., Shao, J., Lin, J., Zhang, N., Lu, B.J., Lin, S.C., Dong, M.Q., and Han, J. (2009). RIP3, an energy metabolism regulator that switches TNF-induced cell death from apoptosis to necrosis. Science *325*, 332-336.

Zhang, Y., Su, S.S., Zhao, S., Yang, Z., Zhong, C.Q., Chen, X., Cai, Q., Yang, Z.H., Huang, D., Wu, R., et al. (2017). RIP1 autophosphorylation is promoted by mitochondrial ROS and is essential for RIP3 recruitment into necrosome. Nat. Commun. *8*, 14329.

Zhao, J., Jitkaew, S., Cai, Z., Choksi, S., Li, Q., Luo, J., and Liu, Z.G. (2012). Mixed lineage kinase domain-like is a key receptor interacting protein 3 downstream component of TNF-induced necrosis. Proc. Natl. Acad. Sci. U. S. A. *109*, 5322-5327.